scientific reports

Check for updates

OPEN

Suppression of LTBP1 enhances the sensitivity of bladder cancer to cisplatin

Zongyang Li[1,6], Yongbo Yu[2,6], Fang Liu[3], Yushu Wu[4], Yunjiang Zang[2], Yanhong Ding[5]✉ & Zhilei Zhang[2]✉

Cisplatin-based chemotherapy is the primary treatment for advanced bladder cancer; however, numerous patients experience treatment failure because of chemoresistance. Therefore, it is crucial to identify drivers of chemoresistance and determine strategies to counteract them to improve prognosis in bladder cancer patients. This study performed proteomics analysis of clinical samples of cisplatin-naïve and resistant bladder cancer tissues. Furthermore, the GEO and TCGA datasets were integrated, which revealed latent transforming growth factor β binding protein 1 (LTBP1) as a potential gene associated with chemoresistance in bladder cancer. LTBP1 expression was correlated with clinical stage and patient survival. LTBP1 knockdown in bladder cancer cells inhibited proliferation, migration, invasion, and chemoresistance *via* TGF-β-mediated epithelial-mesenchymal transition. Subcutaneous tumor and lung metastasis mouse models revealed that LTBP1 inhibition combined with cisplatin treatment significantly inhibited tumor growth and metastasis. Higher LTBP1 expression is associated with a worse prognosis and advanced stage in bladder cancer patients. In conclusion, this study revealed that LTBP1 may be a potential target for alleviating chemoresistance in bladder cancer.

Keywords LTBP1, Chemotherapy resistance, Bladder cancer, EMT

Bladder cancer is one of the most common and deadly urologic cancers, posing significant problems for prevention and treatment[1]. The literature has indicated that about 75% of bladder cancer cases are first identified as non-muscle-invasive bladder cancer (NMIBC)[2]. Patients with NMIBC are susceptible to tumor recurrence post-treatment and may advance to muscle-invasive bladder cancer (MIBC)[3,4]. Currently, the standard treatment for MIBC is neoadjuvant chemotherapy followed by radical cystectomy, which mainly comprises platinum-based regimens, such as gemcitabine plus cisplatin (GC). Neoadjuvant chemotherapy with the GC regimen can reduce tumor size and enhance long-term survival in MIBC patients[5]. Furthermore, aside from enfortumab vedotin plus pembrolizumab, GC remains the recommended treatment strategy for metastatic urothelial carcinoma of the bladder in patients who can tolerate cisplatin[6–8]. However, irrespective of the chemotherapy regimen, drug resistance inevitably develops over time, a major challenge in cancer treatment that can result in therapeutic failure. Despite comprehensive interventions, the 5-year survival rate for MIBC patients remains unsatisfactory at approximately 50%[9], which is closely related to chemoresistance in tumors. Therefore, it is crucial to identify mechanisms of chemoresistance to provide novel theoretical evidence for bladder cancer drug therapy and personalized chemotherapy regimens.

Latent transforming growth factor β binding protein 1 (LTBP1) is a large multidomain protein that belongs to the family of latent TGF-β binding proteins (LTBPs). It is the primary component of the extracellular matrix (ECM)[10]. LTBP1 modulates TGF-β activity indirectly by interacting with the ECM, hence affecting TGF-β's secretion, activation, and functional expression[11,12]. The literature has reported that LTBP1 is significantly related to tumor occurrence, development, and drug resistance *via* various mechanisms (such as TGF-β signaling regulation), as well as epithelial-mesenchymal transition (EMT) processes and tumor microenvironment (TME) modulation[13–15]. However, the role of LTBP1 in bladder cancer remains elusive.

[1]Department of Urology, West Coast Second Hospital of Qingdao University Medical Group, Qingdao 266499, China. [2]Department of Urology, The First Affiliated Hospital of Shandong Second Medical University, Weifang 261041, China. [3]Department of Cardiology, The First Affiliated Hospital of Shandong Second Medical University, Weifang 261041, China. [4]School of Clinical Medicine, Shandong Second Medical University, Weifang 261041, China. [5]Department of Oncology, The First Affiliated Hospital of Shandong Second Medical University, Weifang 261041, China. [6]Zongyang Li and Yongbo Yu contributed equally to this work. ✉email: rmyydingyh@sdsmu.edu.cn; yiyuanzhangzhilei@163.com

This study performed proteomics analysis using public databases and identified LTBP1 as a key gene associated with chemoresistance in bladder cancer. Furthermore, the role and specific molecular mechanisms of LTBP1 in chemoresistance were also evaluated. The data revealed that LTBP1 promoted bladder cancer progression and chemoresistance *via* TGF-β-mediated EMT. LTBP1 was found to be related to the clinical staging and prognosis of bladder cancer patients. LTBP1 knockdown increased bladder cancer cells' sensitivity to chemotherapy. Overall, this study revealed the relationship between LTBP1 and chemoresistance and identified that LTBP1 knockdown increases chemotherapy sensitivity in bladder cancer, thus providing a promising therapeutic target for bladder cancer.

Materials and methods

Tissue samples and cell culture

Pathological specimens of primary and recurrent bladder tumors from 5 cases each, who underwent trimodality therapy (TMT) at the First Affiliated Hospital of Shandong First Medical University between January 2020 and December 2023 were collected. TMT refers to bladder-preserving therapy that combines maximal transurethral resection of bladder tumor with concurrent chemoradiotherapy. Concurrent chemoradiotherapy regimen: cisplatin 40 mg/m^2/week, throughout the radiotherapy; prophylactic irradiation of the entire bladder and pelvic lymphatic drainage areas at 45 Gy/1.8 Gy/25 times, concurrent local bladder tumor and concurrent pelvic metastatic lymph nodes at 60 Gy/2.4 Gy/25 times. The inclusion criterion included surgically resected bladder cancer tissue from patients who had not received other anti-tumor treatments. The samples were preserved in tissue-saving solution for data independent acquisition (DIA) relative quantitative proteomics analysis. The bladder urothelial carcinoma diagnosis was confirmed in all the tissue samples by hospital pathologists. The signed informed consent forms were acquired from patients or their families before the samples were collected. The study was approved by the Research Ethics Committee of The First Affiliated Hospital of Shandong Second Medical University (KYLL20240530-1). Furthermore, for in vitro analysis, T24, J82, UMUC3, and SV-HUC-1 cell lines were acquired from the Chinese Academy of Sciences Cell Bank. All the cells were cultured in DMEM (Gibco, China) containing 10% FBS and 1% penicillin-streptomycin at 37 °C in 5% CO_2.

DIA quantitative proteomics

Briefly, each sample was snap frozen with liquid nitrogen, ground, mixed with an appropriate amount of SDT buffer, transferred to an EP tube, boiled in water for 3 min, sonicated in an ice bath for 2 min, and then centrifuged at 16,000 g and 4℃ for 20 min to acquire supernatant (protein solution). The proteins were quantified using BCA, mixed (15 μg protein) with 5X loading buffer, and boiled in water for 5 min. The proteins were then subjected to 8–16% SDS-PAGE. Protein from each sample was then employed for FASP enzymatic hydrolysis, respectively. An appropriate number of peptide segments were taken from each sample for chromatographic separation, which was performed using the Vanquish Neo UHPLC system and Neo UHPLC (Thermo Scientific). Subsequently, all mass spectrometry data were merged through the software DIA-NN. Then, mass spectrometry data were retrieved from the uniprot-Homo sapiens (Human) [9606]-207981-20230717.fasta (https://www.uniprot.org/9606) database, and quantitative analysis of protein was completed.

Bioinformatics analysis

GEO database analysis: using the GEO database (https://www.ncbi.nlm.nih.gov/geo/), data on chemotherapy-resistant bladder cancer cell lines were searched, and GSE171537 was ultimately selected. Data processing and differential analysis were conducted using R software, with the R packages GEOquery and limma. A significance threshold of 0.05 ($p < 0.05$) was applied, and |Log2 FC| > 1 was considered standard. Differentially expressed genes between the chemotherapy-resistant group and the chemotherapy-sensitive group were identified.

Multivariate COX regression analysis: clinical prognosis data of bladder cancer (BLCA) was obtained from the TCGA database and analyzed using R software, with the R packages survival, forestplot, and tidyverse. First, genes significantly associated with clinical prognosis ($p < 0.01$) were screened. The selected genes were then included in a multivariate COX regression analysis to construct a prognostic model.

Western blot (WB) analysis

The extracted proteins were resolved on 10% SDS–PAGE, transferred to PVDF membranes (Millipore), blocked with a protein-free rapid buffer for 10 min at room temperature, and then treated overnight at 4 °C with primary antibodies against LTBP1 (A15287, ABclonal), Vimentin (60330-1-Ig, Proteintech), E-cadherin (60335-1-Ig, Proteintech), N-cadherin (66219-1-Ig, Proteintech), β-actin (66009-1-Ig, Proteintech), TGF-β (21898-1-AP, Proteintech), Caspase-3 (A2156, ABclonal), and BAX (A0207, ABclonal). The membrane was then washed with TBST thrice and probed with HRP-conjugated secondary antibodies for 1 h at ambient temperature. Protein bands were detected using ECL (Thermo) and quantified *via* the ImageJ software.

Cell proliferation and colony formation assays

CCK8 assay: Cells (1000/well) were seeded in 96-well plates and cultured in 10% FBS-DMEM at 37℃ for 1, 2, and 3 days. Then, 10 μL of CCK-8 reagent was added per well, and absorbance was measured at 450 nm ($n = 3$).

Colony formation analysis: Cells (500/well) were grown in 6-well plates for 14 days. The cells were then fixed with 4% paraformaldehyde for 15 min and stained using 0.1% crystal violet for 3 min. Finally, the cell colonies were analyzed and counted.

Transwell migration and invasion assays

The 24-well transwell chamber is used to study cell migration and invasion. After digestion and centrifugation, resuspend the cells in serum-free medium. A 100 μL cell suspension with a density of 1×10^5 cells/mL was

placed in the upper chamber and 500 µL of DMEM containing 10% FBS was added to the lower chamber. For invasion, add 2 mg/ml matrigel (Corning biocoat 356234) to the bottom of the upper chamber. After 36 h of incubation, the cells were fixed in 4% polyoxymethylene for 15 min and stained with 0.1% crystal violet solution for 15 min. Cells are observed under a light microscope, three randomly selected fields of view are counted and photographed. Each sample was analyzed in triplicate.

Apoptosis assays

The FITC Annexin V apoptosis detection kit (556570, BD Biosciences) was used to assess the cell apoptosis rate through flow cytometry. Briefly, cells were stained with FITC-Annexin V and propidium iodide as per the provided instructions, followed by flow cytometry analysis (FACS, BD Biosciences). The apoptosis rate was calculated by combining the values of early and late apoptotic cells. Data analysis was conducted using FlowJo software (FlowJo_v10.8.1).

Xenograft model

Subcutaneous tumor model: BALB/c nude mice (age: 4 weeks, female, purchased from Beijing Vital River Laboratory Animal Technology Co., Ltd., China) were used. T24-NC and T24-shLTBP1 cells were harvested, counted, and resuspended in 100 µL PBS; 5×10^6 cells were injected subcutaneously into the medial left hind limb. Animals were allocated to four groups: NC, shLTBP1, NC + Cis and shLTBP1 + Cis. Tumor formation was monitored from day 7. Mice in the cisplatin arms received intraperitoneal cisplatin (2.5 mg/kg, twice weekly for 4weeks); control arms received equivalent volumes of saline. Body condition and tumor size were checked every 3 days. Tumor length (L) and width (W) were measured with calipers, and volume was calculated as $(L \times W^2)/2$. After 4 weeks, mice were euthanized using cervical dislocation, tumors were excised intact, and final volumes were analyzed.

Lung metastasis model: BALB/c nude mice (4 weeks, females) were infused via the tail vein with 5×10^5 cells (T24-NC or T24-shLTBP1) in 100 µL PBS. Four groups were established: NC, shLTBP1, NC + Cis, and shLTBP1 + Cis. After 1 week, the cisplatin arms received intraperitoneal cisplatin (2.5 mg/kg, twice weekly for 3 weeks), while controls received equal volumes of saline. At 5 weeks after injection, mice were anesthetized with isoflurane in O_2/N_2O (1:1) and imaged on a Bruker 7 T BioSpec 70/20 USR scanner to assess pulmonary metastases. Animals were then euthanized using cervical dislocation; lungs were excised, fixed, and processed for HE staining. Metastatic foci in each lung were enumerated.

The animal experiments in this study have been approved by the Laboratory Animal Center of Shandong Second Medical University, with the ethics review approval number: 2023SDL338.

Immunohistochemistry (IHC) analysis

Slides with cultured cells were deparaffinized in xylene, rehydrated through graded ethanol (100, 95, 90, 80, and 70%), and subjected to antigen retrieval using 10 mM sodium citrate (pH 6.0) with blocking serum. Then, the slides were probed with primary antibody (A15287, ABclonal) overnight at 4 °C, followed by biotinylated secondary antibody. DAB (Servicebio) was employed to develop protein signals. Cell staining intensity was scored from 1 to 3, where 1 indicated no or weak staining, 2 depicted moderate staining, and 3 showed strong staining. The percentage of positive cells was scored as 1 (0–25%), 2 (25–50%), 3 (50–75%), and 4 (75–100%). The final score of the sample is obtained by multiplying the two scores.

Statistical analysis

Statistical analyses were carried out with SPSS 26.0 (IBM), GraphPad Prism, and R 4.3.1 (https://www.r-project.org/). Two-tailed t-tests were carried out for inter-group comparison, whereas one-way ANOVA was performed for multiple groups comparison. The association between the clinicopathological characteristics of the two groups were assessed using Fisher's exact test. Overall survival was estimated using Kaplan–Meier curves. $p < 0.05$ was deemed statistically significant.

Results

Proteomics revealed that differentially expressed proteins (DEPs) were associated with bladder cancer chemoresistance

The heat map of proteomics showed differences in protein expression between the two groups (Fig. 1A). The t-tests combined with fold change (the ratio of average expression levels between two groups, FC) were performed to analyze significantly different proteins ($p < 0.05$, FC ≥ 1.5, or ≤ 1/1.5), which revealed 828 DEPs (513 upregulated and 315 downregulated) in the chemoresistant group (Fig. 1B). GO functional enrichment analysis revealed that these DEPs were primarily enriched in the following biological processes (BP): immune system processes, cell migration, and cell movement (Fig. 1C). Furthermore, they were significantly associated with various cell components (CC), including cytoplasm, cell periphery, and cytoplasmic components in the category (Fig. 1D). The primary molecular function (MF) associated with these DEPs included nucleoside triphosphatase regulatory activity, GTPase regulatory activity, and actin binding (Fig. 1E). KEGG pathway enrichment analysis indicated that these DEPs were primarily enriched in chemokine signaling pathways, Rap1 signaling pathways, and cGMP-PKG signaling pathways (Fig. 1F).

LTBP1 was identified as a prospective gene related to chemoresistance in bladder cancer

The GEO database analysis of cisplatin-resistant and chemosensitive bladder cancer cell lines (GSE171537) data identified 2,079 DEPs through differential analysis (Fig. 2A). The DEPs from proteomics data and the GEO database were intersected, and the duplicates were removed, which revealed 85 genes associated with chemoresistance in bladder cancer (Fig. 2B). Subsequently, Cytoscape was employed to construct a protein-

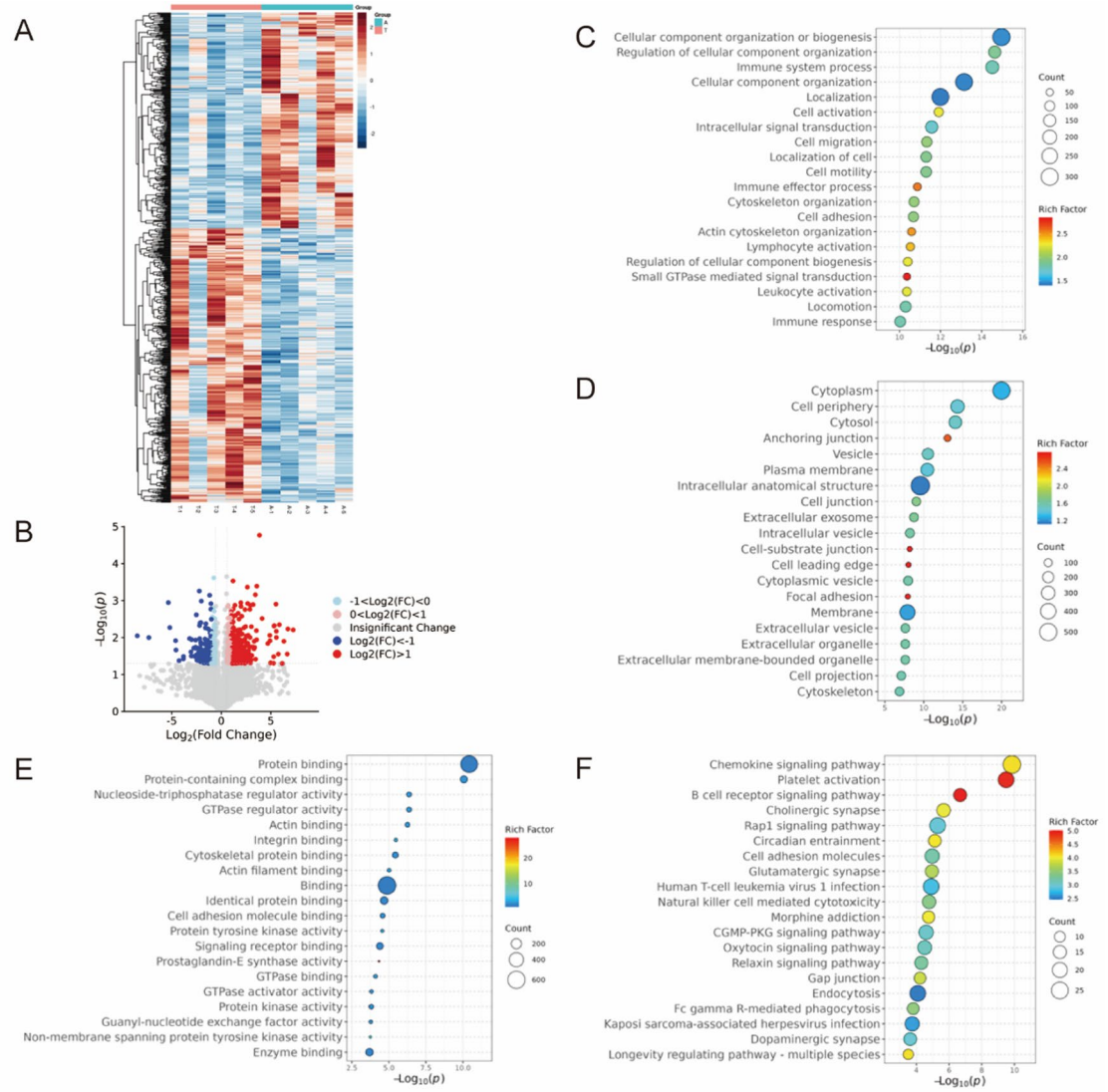

Fig. 1. Proteomics revealed that differentially expressed proteins (DEPs) were associated with bladder cancer chemoresistance. **(A)** Cluster heat map of differential proteins. The redder the color, the higher the relative expression, and the bluer the lower the relative expression. **(B)** Volcanic diagram of differential proteins. Each dot represents a protein, with red dots for significantly high expression proteins, blue dots for significantly low expression proteins, and gray dots for non-differential proteins. **(C)** BP term enrichment bubble diagram of differential proteins (top20). **(D)** MF term enrichment bubble diagram of differential proteins (top20). **(E)** BP term enrichment bubble diagram of differential proteins (top20). **(F)** KEGG pathway enrichment bubble diagram of differential proteins (top20; source: www.kegg.jp/kegg/kegg1.html).

protein interaction (PPI) network for chemoresistance-related genes, which identified LTBP1 as a core candidate protein (Fig. 2C). Clinical prognosis data for bladder cancer from the TCGA database were analyzed using R software to identify genes substantially correlated with clinical outcomes, which were subsequently incorporated into a multivariate Cox regression analysis to develop a prognostic model (Fig. 2D). The results showed that LTBP1 is a prognostic risk factor for bladder cancer patients. Furthermore, the TCGA database analysis revealed that LTBP1 expression was linked to bladder cancer patient prognosis, with higher LTBP1 expression associated with a worse prognosis (Fig. 2E). Moreover, LTBP1 expression was related to T stage and clinical stage of bladder cancer (Fig. 2F). As these stages progress, LTBP1 expression increases. Overall, it was inferred that LTBP1 is a potential gene that modulates cisplatin chemoresistance in bladder cancer.

LTBP1 promoted the progression of bladder cancer through TGF-β

The WB analysis of proteins extracted from bladder cancer cell lines (T24, UMUC3, and J82) and normal human urothelial cells (SV-HUC-1) revealed higher LTBP1 expression in cancer cells (Fig. 3A). Furthermore, WB assay was carried out to validate the knockdown of LTBP1 in T24 and UMUC3 cell lines after using siRNA for LTBP1 silencing (Fig. 3B). Then, functional experiments were performed, in which CCK8 assay showed that inhibition of LTBP1 significantly reduced the short-term viability and proliferation of bladder cancer cells;

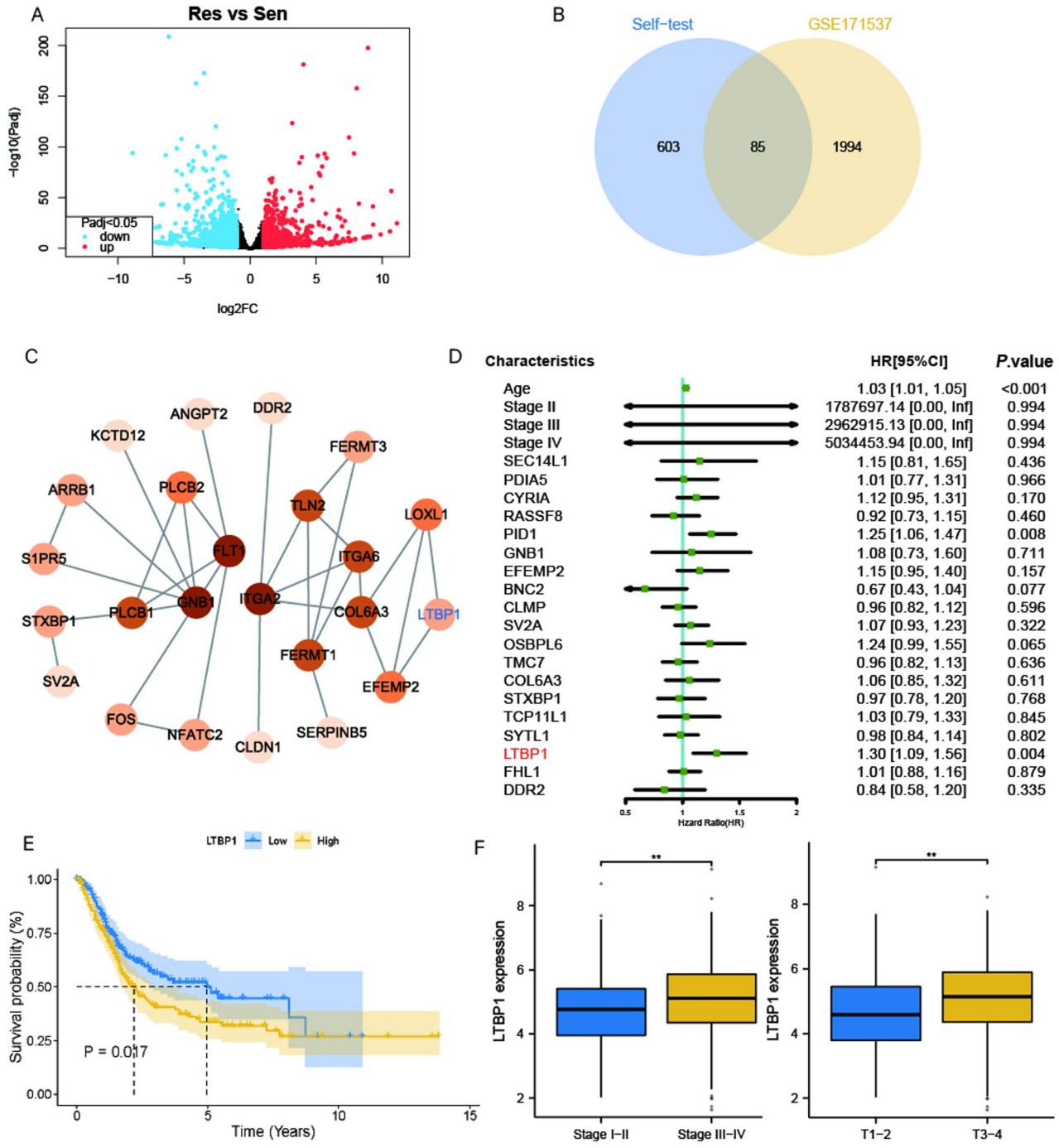

Fig. 2. LTBP1 was identified as a prospective gene related to chemoresistance in bladder cancer. **(A)** Volcanic diagram of the differential proteins of the GSE171537. **(B)** Venn plot of differential genes in both proteomics and GEO database. **(C)** PPI network of genes related to chemotherapy resistance. **(D)** Multifactorial COX regression forest diagram. **(E)** Survival analysis of bladder cancer patients with different LTBP1 expression levels. **(F)** Correlation analysis between clinical stage as well as T stage and LTBP1 expression in bladder cancer patients. $^{**}p < 0.01$.

however, this effect can be reversed with TGF-β (Fig. 3C). Moreover, the transwell assay revealed that LTBP1 knockdown inhibited cell migration and invasion activity (Fig. 3D). Mechanically, LTBP1 knockdown reduced EMT-related proteins N-Cadherin and Vimentin, an effect reversed by TGF-β (Fig. 3E). For further research, we also employed lentivirus-mediated infection to establish stable LTBP1-knockdown T24 and UMUC3 cell lines. Consistently, these stable cell lines indicated reduced levels of N-Cadherin, Vimentin, and TGF-β, while increased expression of E-Cadherin (Fig. 3F). To speculate on the effect of LTBP1 on tumorigenesis, colony formation assay was carried out, which demonstrated that LTBP1 knockdown inhibited clonal formation

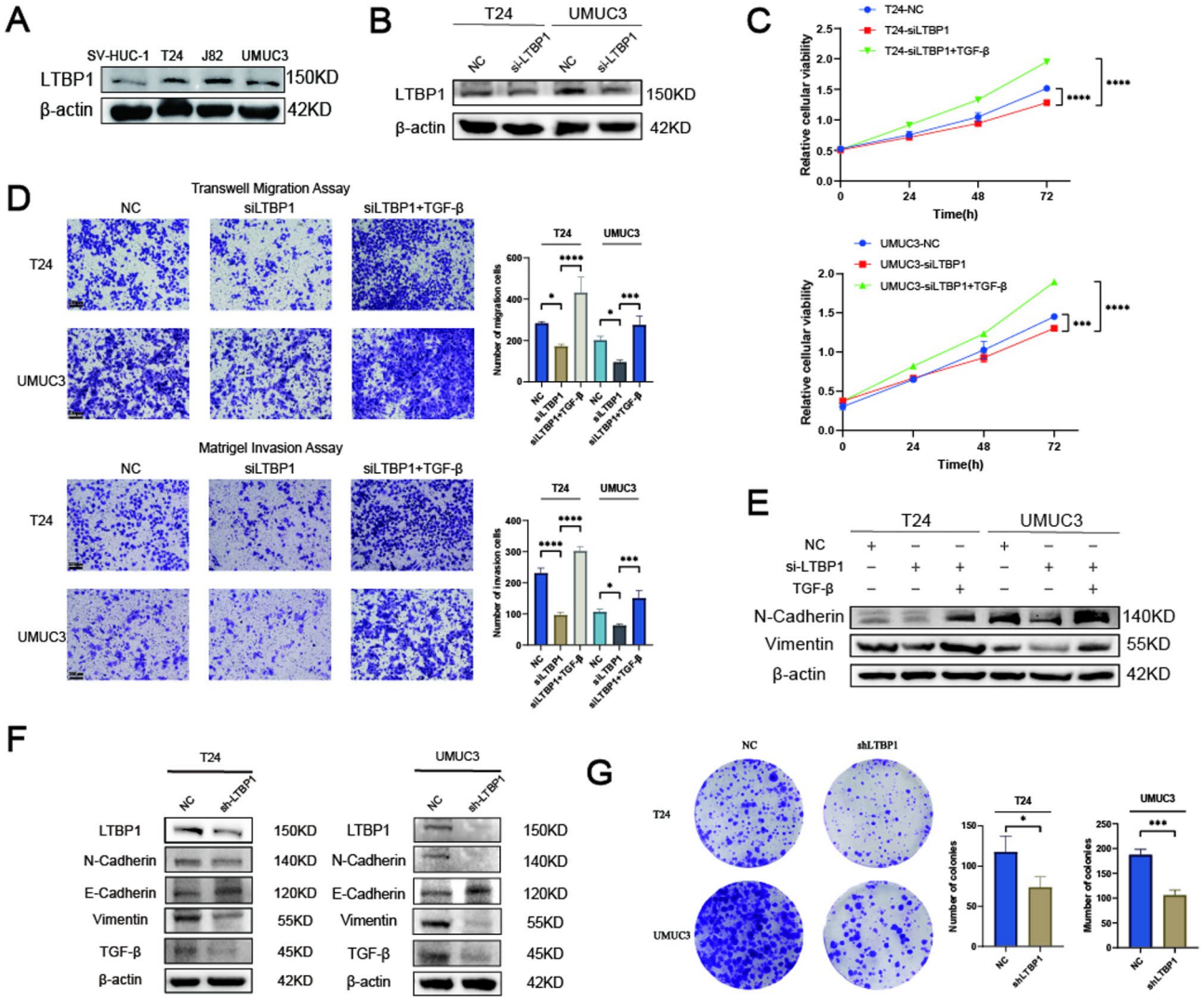

Fig. 3. LTBP1 promoted the progression of bladder cancer through TGF-β.. **(A)** The expression level of LTBP1 in T24, J82, and UMUC3 cells is higher than that in SV-HUC1 cells. **(B)** SiRNA knocked down LTBP1 expression levels in T24 and UMUC3 cells. **(C)** CCK8 test results for different groups at time intervals of 0, 24, 48, and 72 h. **(D)** Photographic and statistical analysis of Transwell cell migration and invasion experiments. The knockdown of LTBP1 inhibited the migration and invasion of T24 and UMUC3 cells, while the addition of TGF-β still enhanced cell migration and invasion. Scale bar = 200 μm. **(E)** Knockdown of LTBP1 expression in T24 and UMUC3 cells led to a decrease in the expression levels of N-Cadherin and Vimentin, and the addition of TGF-β significantly reversed the expression. **(F)** Compared with NC group, the expression levels of N-Cadherin, Vimentin and TGF-β in the sh-LTBP1 group of T24 and UMUC3 cells were decreased, and the expression levels of E-Cadherin were increased. **(G)** Photographic and statistical analysis of colony formation assay. The number of clonal formation was significantly reduced after LTBP1 knockdown. *$p < 0.05$, ***$p < 0.001$, ****$p < 0.0001$.

(Fig. 3G). These results suggested that LTBP1 could promote the proliferation, migration and invasion of bladder cancer cells by activating its downstream factor TGF-β.

LTBP1 knockdown enhanced chemosensitivity in bladder cancer

To investigate the molecular mechanism of LTBP1 in bladder cancer chemoresistance, LTBP1 protein expression before and during cisplatin treatment was evaluated. Results indicated that cisplatin elevated LTBP1 expression and augmented TGF-β secretion (Fig. 4A). We found that knockdown of LTBP1 in bladder cancer cells significantly reduced the IC50 value of cisplatin, indicating increased chemotherapy sensitivity (Fig. 4B). Besides, flow cytometry was used to investigate the effect of LTBP1 on bladder cell apoptosis. We found that LTBP1 knockdown increased apoptosis rates in T24 and UMUC3 cells, and this pro-apoptotic effect was synergistically enhanced by cisplatin (Fig. 4C, D). Moreover, in LTBP1-knockdown cells, the expression of apoptosis markers BAX and Caspase3 was upregulated, which was further increased after cisplatin treatment

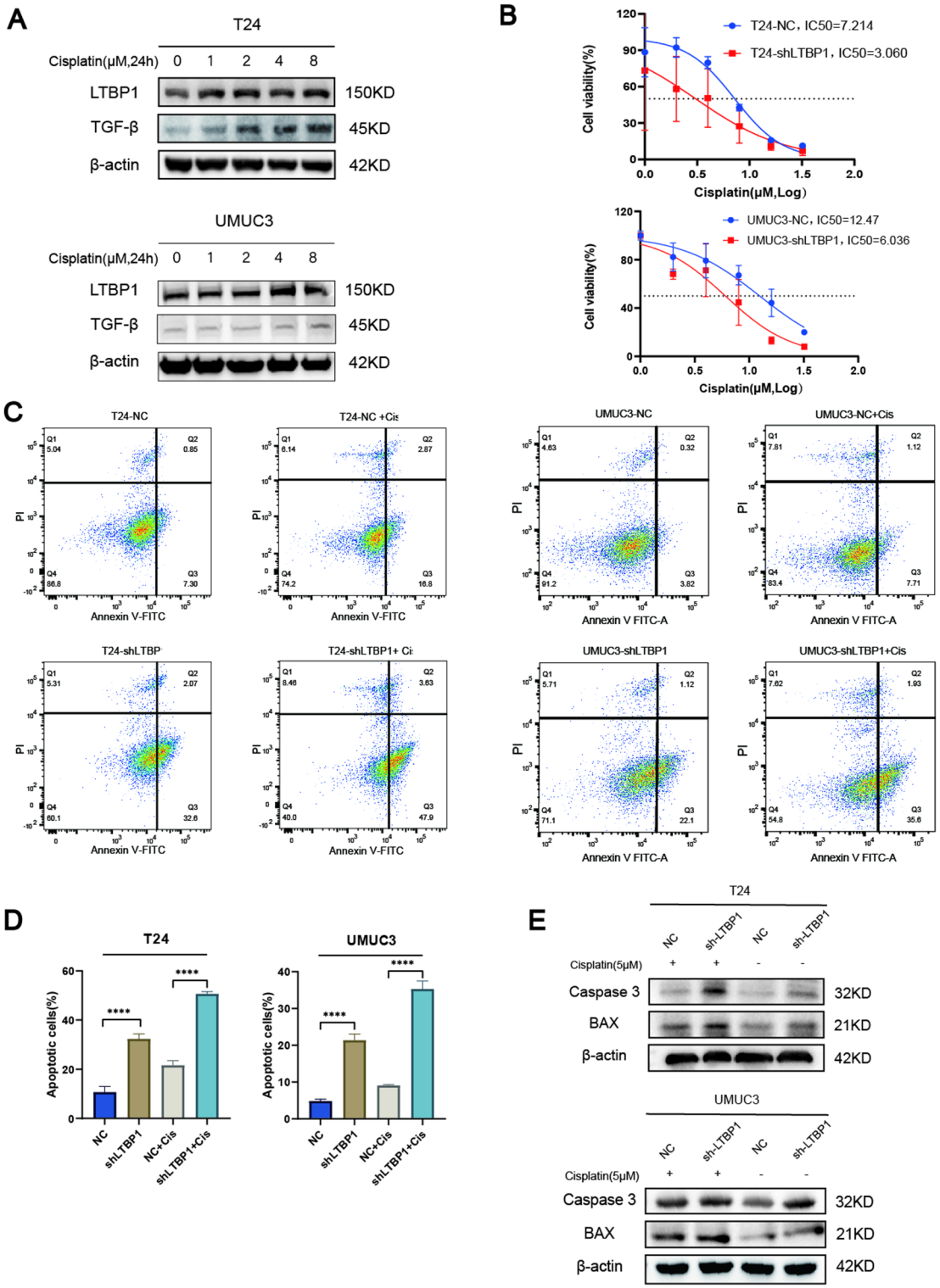

Fig. 4. LTBP1 knockdown enhanced chemosensitivity in bladder cancer. (**A**) The expression level of LTBP1 in bladder cancer cells increased after cisplatin treatment, and TGF-β secretion was up-regulated with the change of cisplatin dose. (**B**) Experimental results of CCK8 in different groups. The IC50 value of cisplatin decreased in cells after LTBP1 knockdown. (**C**) Apoptosis in different groups. (**D**) Statistical analysis of the apoptosis rates in different cell groups. (**E**) WB analysis of Caspase 3, BAX and β-actin in differren cell groups. $^{****}p < 0.0001$.

(Fig. 4E). Taken together, we suggested that inhibition of LTBP1 could improve cisplatin chemoresistance by promoting apoptosis.

LTBP1 knockdown inhibited tumor growth and lung metastasis in vivo

Xenograft assays on subcutaneous tumor-bearing and lung metastasis mouse models were conducted to evaluate the impact of LTBP1 knockdown on tumor growth and lung metastasis in vivo. The data showed that the shLTBP1 group of subcutaneous tumor-bearing models had smaller tumor volumes than the NC group, while the shLTBP1 + cisplatin group had the smallest tumor volumes (Fig. 5A, B), with no obvious toxic side effects (Fig. 5C). This demonstrated that LTBP1 silencing inhibited tumor growth in vivo, with the most pronounced anticancer effect observed when LTBP1 knockdown was paired with cisplatin. Furthermore, for the in vivo metastasis analysis, the lungs of mice were scanned using MRI to observe lung metastatic nodules (Fig. 5D, E). Then, the lung specimens from the mice were obtained for hematoxylin and eosin staining (Fig. 5F). In comparison to the NC group, mice administered T24-shLTBP1 cells had a reduced number of lung metastatic nodules, with the most pronounced suppression of lung metastasis observed in the shLTBP1 + cisplatin cohort. Altogether, these results suggested that inhibition of LTBP1 could reduce tumorization and metastasis of bladder cancer cells in vivo.

LTBP1 inhibition indicated a better prognosis for patients with bladder cancer

To explore the relationship between LTBP1 and the prognosis of bladder cancer patients, an IHC assay was performed to observe LTBP1 expression in patients undergoing radical cystectomy. Patients undergoing radical cystectomy all received GC neoadjuvant chemotherapy. Neoadjuvant chemotherapy regimen: Gemcitabine, on days 1 and 8, 1000 mg/m^2, every 21 days for one cycle; Cisplatin, on day 1 or 2, 70 mg/m^2, every 21 days for one cycle. Then, based on the IHC scores of LTBP1, patients were categorized into the higher and lower LTBP1 groups (Fig. 6A). The examination of clinical features subsequently associated increased LTBP1 levels with advanced pathological stages in bladder cancer (Table 1). Furthermore, the association of overall survival with LTBP1 expression was also evaluated, which revealed that patients with elevated LTBP1 levels had a poorer prognosis (Fig. 6B). Furthermore, LTBP1 levels increased with the progression of pathological, T, and N stages of bladder cancer (Fig. 6C-E). These findings showed that LTBP1 not only serves as a diagnostic indicator but also as a therapeutic target in bladder cancer.

Discussion

Cisplatin regimens continue to be the primary treatment for advanced bladder cancer. Neoadjuvant and adjuvant chemotherapy are both extensively utilized and efficacious. However, certain patients experience therapy failure due to chemoresistance. Chemoresistance is a complex phenomenon associated with various genes and signaling pathways[16–18]; therefore, understanding its mechanisms in bladder cancer is crucial for developing targeted interventions. The current known mechanisms of chemoresistance include altered drug targets, increased drug efflux, inhibition of cell death, EMT, apoptosis evasion, abnormal DNA damage/repair, and epigenetic changes[19–21]. LTBP1 is a member of the latent TGF-β-binding protein family and regulates TGF-β secretion and activation[22]. In this study, proteomics and bioinformatics analysis revealed that LTBP1 was differentially expressed in cisplatin-resistant bladder cancer tissues, which is significantly associated with patient prognosis. Therefore, the role of LTBP1 in bladder cancer chemoresistance should be comprehensively investigated.

Previous studies have linked LTBP1 to cancer promotion. For instance, LTBP1 is a potential ovarian cancer biomarker[23]. In tumors, LTBP1 initiates TGF-β signaling, and its silencing reduces TGF-β activity and Smad2 phosphorylation in glioblastoma cells[24,25]. Breast cancer progression has also been linked with LTBP1 *via* the WNT/Ca^{2+}-CaMKII-NF-κB axis[26]. Furthermore, LTBP1 promotes esophageal cancer progression through EMT and cancer-associated fibroblast transformation[27]. Moreover, in gastric cancer, LTBP1 correlates with tumor progression and can predict patient prognosis[28]. However, the function of LTBP1 in bladder cancer remains ambiguous. This study identified an association between LTBP1 and the clinical stage and prognosis of bladder cancer patients. Patients with elevated pathological staging demonstrated increased expression of LTBP1. Elevated LTBP1 levels predicted a more advanced pathological state and poorer prognosis. These findings were consistent with previous studies, indicating that LTBP1 may serve as a diagnostic and prognostic biomarker for bladder cancer.

This study also evaluated the function and molecular mechanisms of LTBP1 in bladder cancer cells. The data revealed that LTBP1 inhibition reduced the proliferation, migration, and invasion of bladder cancer cells. Furthermore, LTBP1 knockdown reduced the expression of TGF-β, a key EMT inducer, which can induce nuclear-related miRNA expression, inducing epithelial cell-specific protein translation and promoting mesenchymal cell-specific protein expression, therefore driving EMT[29,30]. Furthermore, TGF-β can increase the transcription and translation of EMT-related genes *via* the noncanonical pathways, such as the oncogenic RAS-MAPK pathway[31,32]. LTBP1 knockdown reduced N-cadherin and vimentin levels, while increasing E-cadherin expression. These data showed that LTBP1 modulates TGF-β release and activation, thus driving EMT in bladder cancer. Furthermore, the rescue experiment demonstrated that after LTBP1 expression, an upstream signal for TGF-β, TGF-β could still exert its effects. The aforementioned results indicated that LTBP1 facilitated the advancement of bladder cancer *via* TGF-β-mediated EMT.

Several studies have indicated that EMT promotes chemoresistance in multiple cancers and may serve as a therapeutic target[33]. This study confirmed that LTBP1 can cause EMT and that LTBP1 inhibition could enhance the sensitivity of bladder cancer cells to cisplatin. Besides, it was observed that cisplatin upregulated LTBP1 and TGF-β in bladder cancer cells. This may activate apoptosis-related signaling pathways, elevate anti-apoptotic proteins, or diminish pro-apoptotic proteins, resulting in an imbalance of apoptosis and chemoresistance. Further research showed that LTBP1 knockdown promoted apoptosis in bladder cancer cells through BAX/

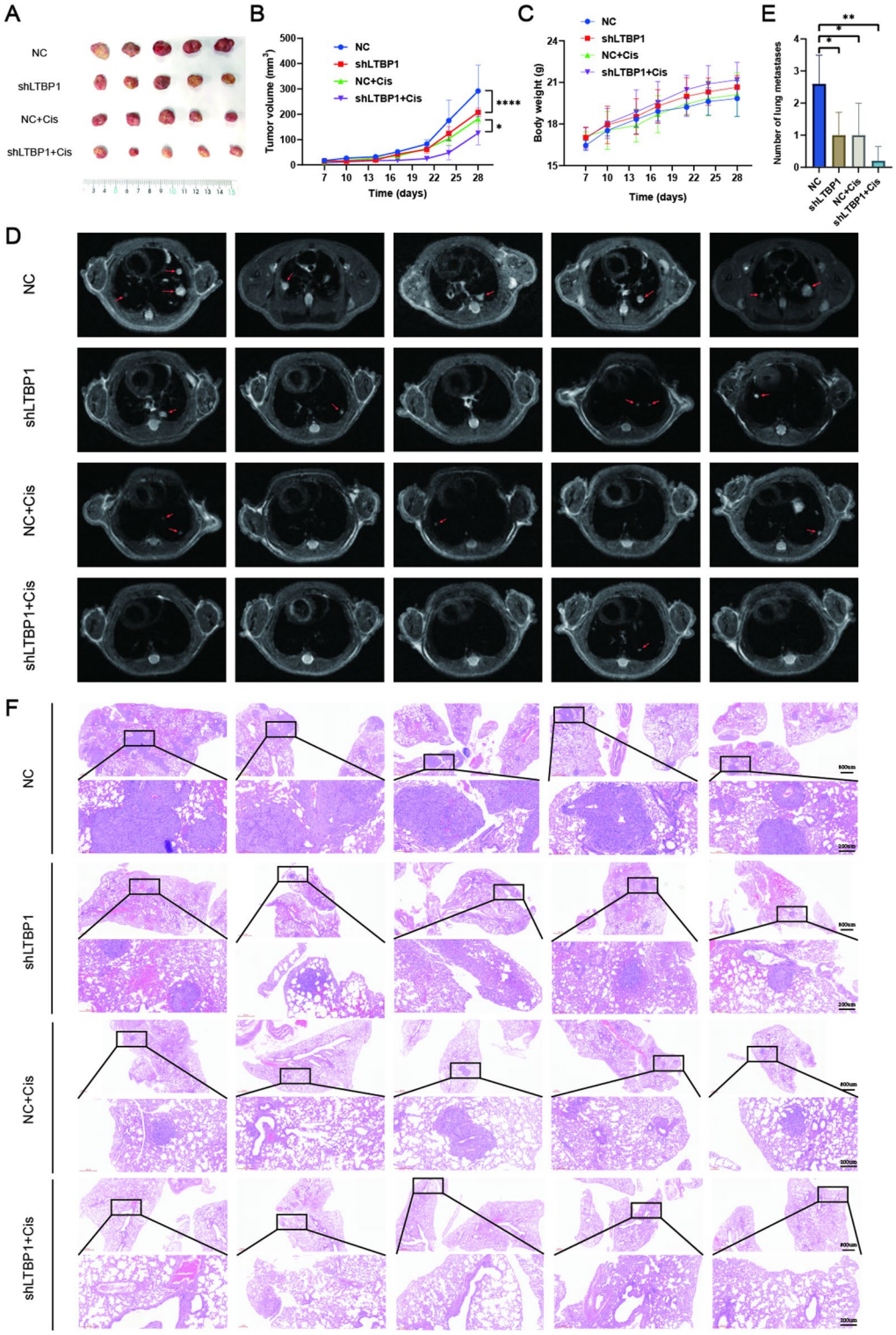

Fig. 5. LTBP1 knockdown inhibited tumor growth and lung metastasis in vivo. **(A)** Comparison of tumor sizes in different groups of mouse subcutaneous tumor-bearing models. (n=5 per group) **(B)** Tumor growth curves of different groups in the subcutaneous tumor models. **(C)** Weight growth curves of subcutaneous tumor models in different groups. **(D)** T2-weighted MRI imaging of lung metastasis models. The red arrows indicated the location of the tumor (n=5 per group). **(E)** Statistical analysis of the number of lung metastases in different groups. **(F)** HE staining of lung tissue in mouse lung metastasis models (2× and 10×). Up: Scale bar = 800 μm. Down: Scale bar = 200 μm. *$p < 0.05$, **$p < 0.01$, ****$p < 0.0001$.

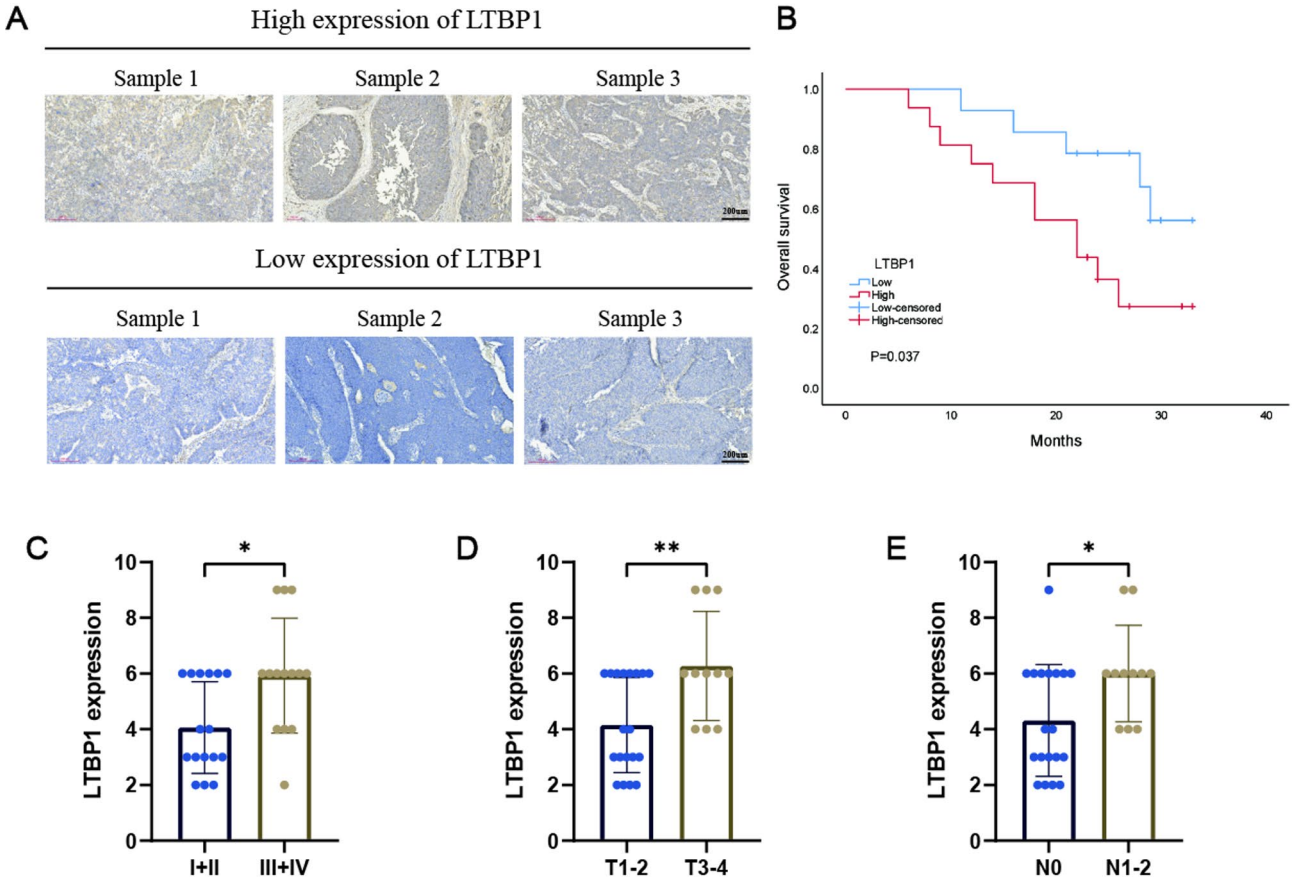

Fig. 6. LTBP1 inhibition indicated a better prognosis for patients with bladder cancer.. (**A**) IHC examples grouped at different LTBP1 expression levels. Scale bar = 200 μm. **(B)** Overall survival curves of patients in different groups. **(C, D, E)** Correlation analysis of LTBP1 expression with clinical stage, T stage and N stage. *$p < 0.05$, **$p < 0.01$.

Caspase3. Animal studies have demonstrated that the inhibition of LTBP1, in conjunction with cisplatin, significantly reduces bladder tumor development and metastasis in vivo. In summary, our study showed that targeted inhibition of LTBP1 could reverse EMT, promote apoptosis, and synergize with cisplatin to significantly suppress tumor growth and metastasis.

Fibronectin, a predominant ECM component, influences tumor cell adhesion, migration, and invasion, and is significantly associated with chemoresistance[34,35]. LTBP1 has been found to promote the transformation of cancer-associated fibroblasts (CAFs) in esophageal cancer and boost CAF-derived fibronectin secretion[27]. CAFs modulate TME by secreting factors such as TGF-β, VEGF, and FGF2 that promote tumor invasion and metastasis[36]. Furthermore, they can also promote TME fibrosis, which is comprised of blood vessels, enhancing interstitial pressure, and causing poor drug penetration[37]. Moreover, CAFs promote M2 macrophage polarization *via* a Snail1-dependent mechanism, reducing their anti-tumor activity and enhancing tumor resistance to chemotherapy and immunotherapy[37]. Therefore, future research should focus on how the TME affects LTBP1 expression and function, as well as the interactions between LTBP1 and TME components to clarify the comprehensive mechanisms of LTBP1-mediated chemoresistance.

There are some shortcomings in this study. For example, the number of clinical samples was not sufficient, and the exploration of mechanisms was not specific enough. We will collect more clinical samples and information to validate our hypothesis.

Conclusion

In summary, this study performed proteomic sequencing of bladder cancer chemoresistant tissue samples. Furthermore, the bioinformatics analysis of the GEO and TCGA databases identified LTBP1 as a key gene associated with chemotherapy resistance. Moreover, LTBP1 expression was found to correlate with poor clinical prognosis in bladder cancer patients. LTBP1 promotes bladder cancer cell proliferation, migration, and invasion, and enhances chemoresistance. Mechanistically, LTBP1 drives tumor progression and chemoresistance via TGF-β-dependent EMT-related pathways.

Characteristics	LTBP1 Expression		*P*
	Low	High	
Cases (n)	14(46.7%)	16(53.3%)	
Age (year)			0.336
<60	1(7.1%)	4(25.0%)	
≥60	13(92.9%)	12(75.0%)	
Gender			1.000
Male	12(85.7%)	14(87.5%)	
Female	2(14.3%)	2(12.5%)	
Tumor size (cm)			0.713
<4	7(50.0%)	6(37.5%)	
≥4	7(50.0%)	10(62.5%)	
Pathology grade			1.000
Low	1(7.1%)	1(6.3%)	
High	13(92.9%)	15(93.8%)	
AJCC			0.024
Ⅰ	5(35.7%)	1(6.3%)	
Ⅱ	6(42.9%)	4(25.0%)	
Ⅲ	3(21.4%)	11(68.8%)	
T stage			0.142
T1-2	11(78.6%)	8(50.0%)	
T3-4	3(21.4%)	8(50.0%)	
N stage			1.000
N0	10(71.4%)	12(75.0%)	
N1-2	4(28.6%)	4(25.0%)	

Table 1. Associations between LTBP1 expression and clinical characteristics in bladder cancer patients. AJCC: American Joint Committee on Cancer.

Data availability

The datasets used and analyzed during the current study are available from the corresponding author on reasonable request.

Received: 8 September 2025; Accepted: 27 February 2026
Published online: 13 March 2026

References

1. van Hoogstraten, L. et al. Global trends in the epidemiology of bladder cancer: Challenges for public health and clinical practice. *Nat. Rev. Clin. Oncol.* **20** (5), 287–304 (2023).
2. Lobo, N. et al. Epidemiology, screening, and prevention of bladder cancer. *Eur. Urol. Oncol.* **5** (6), 628–639 (2022).
3. Im, S. W. et al. Genomic landscape of young-onset bladder cancer and its prognostic implications on adult bladder cancer. *Cancers (Basel)* **12**(2), 307 (2020).
4. Venkatesulu, B. et al. Multidisciplinary management and radiotherapy recommendations for clinically and pathologically node-positive bladder cancer. *Semin Radiat. Oncol.* **33** (1), 35–50 (2023).
5. Kim, D. K., Lee, J. Y., Jung, J. H., Hah, Y. S. & Cho, K. S. Role of adjuvant cisplatin-based chemotherapy following radical cystectomy in locally advanced muscle-invasive bladder cancer: Systematic review and meta-analysis of randomized trials. *Investig. Clin. Urol.* **60** (2), 64–74 (2019).
6. van der Heijden, A. G. et al. European Association of Urology guidelines on muscle-invasive and metastatic bladder cancer: Summary of the 2025 guidelines. *Eur. Urol.* **87**, 582–600 (2025).
7. Javier, P. et al. SEOM-SOGUG clinical guideline for urothelial cancer (2025). *Clin. Transl Oncol.* **27**, 4142–4159 (2025).
8. Zhang, F. & Li, S. Antibody-drug conjugates as game changers in bladder cancer: Current progress and future directions. *Front. Immunol.* **16**, 1591191 (2025).
9. Marcos-Gragera, R. et al. Urinary tract cancer survival in Europe 1999–2007: Results of the population-based study EUROCARE-5. *Eur. J. Cancer*. **51** (15), 2217–2230 (2015).
10. Rifkin, D. B., Rifkin, W. J. & Zilberberg, L. LTBPs in biology and medicine: LTBP diseases. *Matrix Biol.* **71–72**, 90–99 (2018).
11. Jackson, J. W. et al. An antibody that inhibits TGF-β1 release from latent extracellular matrix complexes attenuates the progression of renal fibrosis. *Sci. Signal.* **17** (844), eadn6052 (2024).
12. Rifkin, D. et al. The role of LTBPs in TGF beta signaling. *Dev. Dyn.* **251** (1), 95–104 (2022).
13. Yang, S. et al. LTA4H improves the tumor microenvironment and prevents HCC progression via targeting the HNRNPA1/LTBP1/TGF-β axis. *Cell. Rep. Med.* **6** (3), 102000 (2025).
14. Zhao, Q. et al. PTPS facilitates compartmentalized LTBP1 S-nitrosylation and promotes tumor growth under hypoxia. *Mol. Cell.* **77** (1), 95–107e5 (2020).
15. Morini, M. et al. Plasma-derived exosome proteins as novel diagnostic and prognostic biomarkers in neuroblastoma patients. *Cells* **12**(21). (2023).
16. Lin, X. et al. N(6)-methyladenosine modification of CENPK mRNA by ZC3H13 promotes cervical cancer stemness and chemoresistance. *Mil Med. Res.* **9** (1), 19 (2022).

17. Tian, W. et al. Extracellular vesicles in ovarian cancer chemoresistance, metastasis, and immune evasion. *Cell. Death Dis.* **13** (1), 64 (2022).
18. Zhang, Y. et al. Epiregulin increases stemness-associated genes expression and promotes chemoresistance of non-small cell lung cancer via ERK signaling. *Stem Cell. Res. Ther.* **13** (1), 197 (2022).
19. Hraběta, J. et al. Drug sequestration in lysosomes as one of the mechanisms of chemoresistance of cancer cells and the possibilities of its inhibition. *Int. J. Mol. Sci.* **21** (12), 4392 (2020).
20. Novoa Díaz, M. B., Martín, M. J. & Gentili, C. Tumor microenvironment involvement in colorectal cancer progression via Wnt/β-catenin pathway: Providing understanding of the complex mechanisms of chemoresistance. *World J. Gastroenterol.* **28** (26), 3027–3046 (2022).
21. Vaghari-Tabari, M. et al. CRISPR/Cas9 gene editing: A new approach for overcoming drug resistance in cancer. *Cell. Mol. Biol. Lett.* **27** (1), 49 (2022).
22. Singh, K., Sachan, N., Ene, T., Dabovic, B. & Rifkin, D. Latent transforming growth factor β binding protein 3 controls adipogenesis. *Matrix Biol.* **112**, 155–170 (2022).
23. Wenk, D. et al. Targeted mass spectrometry of longitudinal patient sera reveals LTBP1 as a potential surveillance biomarker for high-grade serous ovarian carcinoma. *J. Proteome Res.* **23** (2), 749–759 (2024).
24. Liao, J. et al. Cross-talk between the TGF-β and cell adhesion signaling pathways in cancer. *Int. J. Med. Sci.* **21** (7), 1307–1320 (2024).
25. Zhang, Q. et al. Tibetan mesenchymal stem cell-derived exosomes alleviate pulmonary vascular remodeling in hypoxic pulmonary hypertension rats. *Stem Cells*. **42** (8), 720–735 (2024).
26. Spina, E. & Cowin, P. Embryonic mammary gland development. *Semin Cell. Dev. Biol.* **114**, 83–92 (2021).
27. Cai, R. et al. LTBP1 promotes esophageal squamous cell carcinoma progression through epithelial-mesenchymal transition and cancer-associated fibroblasts transformation. *J. Transl Med.* **18** (1), 139 (2020).
28. Jiang, X. et al. A prognostic marker LTBP1 is associated with epithelial mesenchymal transition and can promote the progression of gastric cancer. *Funct. Integr. Genomics*. **24** (1), 30 (2024).
29. Lee, J. H. & Massagué, J. TGF-β in developmental and fibrogenic EMTs. *Semin Cancer Biol.* **86** (Pt 2), 136–145 (2022).
30. Wang, X., Eichhorn, P. & Thiery, J. P. TGF-β, EMT, and resistance to anti-cancer treatment. *Semin Cancer Biol.* **97**, 1–11 (2023).
31. Peng, D., Fu, M., Wang, M., Wei, Y. & Wei, X. Targeting TGF-β signal transduction for fibrosis and cancer therapy. *Mol. Cancer*. **21** (1), 104 (2022).
32. Zhang, Y. E. & Stuelten, C. H. Alternative splicing in EMT and TGF-β signaling during cancer progression. *Semin Cancer Biol.* **101**, 1–11 (2024).
33. Dart, A. EMT in chemoresistance. *Nat. Rev. Cancer*. **23** (6), 349 (2023).
34. Farooq, F., Amin, A., Wani, U. M., Lone, A. & Qadri, R. A. Shielding and nurturing: Fibronectin as a modulator of cancer drug resistance. *J. Cell. Physiol.* **238** (8), 1651–1669 (2023).
35. Qiao, P. & Lu, Z. R. Fibronectin in the tumor microenvironment. *Adv. Exp. Med. Biol.* **1245**, 85–96 (2020).
36. Xiao, Y. & Yu, D. Tumor microenvironment as a therapeutic target in cancer. *Pharmacol. Ther.* **221**, 107753 (2021).
37. Agosti, E. et al. Tumor microenvironment and glioblastoma cell interplay as promoters of therapeutic resistance. *Biology (Basel)*. **12** (5), 736 (2023).

Acknowledgements

We express our gratitude for the experimental platform provided by the Laboratory Animal Center of Shandong Second Medical University.

Author contributions

Zhilei Zhang and Yanhong Ding conceptualized and supervised this study. Zongyang Li performed the experiments, wrote the manuscript and prepared figures. Yongbo Yu performed the experiments, analyzed the data and prepared figures. Fang Liu and Yushu Wu performed proteome and bioinformatics analysis. Yunjiang Zang prepared the table. All authors read and approved the final manuscript. ZL and YY made equal contributions as co-first authors. ZZ and YD are co-corresponding authors responsible for interpreting communications.

Funding

This work was financially supported by Postdoctoral Innovation Program of Shandong Province (SDCX-ZG-202502104), Scientific Research Development Fund Project of Shandong Second Medical University Affiliated Hospital (2024FYQ022), Weifang Science and Technology Development Plan Project (2024YX014).

Declarations

Competing interests

The authors declare no competing interests.

Ethics approval

The study was approved by the Research Ethics Committee of The First Affiliated Hospital of Shandong Second Medical University (KYLL20240530-1) and complied with the rules of the Declaration of Helsinki principles. The animal experiments were approved by the Laboratory Animal Center of Shandong Second Medical University (2023SDL338). All animal procedures were conducted according with international guidelines and the Basel Declaration. We complied with the ARRIVE guidelines.

Additional information

Supplementary Information The online version contains supplementary material available at https://doi.org/10.1038/s41598-026-42815-2.

Correspondence and requests for materials should be addressed to Y.D. or Z.Z.